Photoaffinity Labeling of Cytochrome P450 2B4: Capture of Active Site Heme Ligands by a Photocarbene†

John P. Miller‡,§ and Ronald E. White*,‖

Department of Pharmacology, University of Connecticut Health Center, Farmington, Connecticut 06030, and Department of Metabolism and Pharmacokinetics, Bristol-Myers Squibb Pharmaceutical Research Institute, P.O. Box 4000, Princeton, New Jersey 08543-4000

Received August 6, 1993; Revised Manuscript Received November 10, 1993•

ABSTRACT: Spiro[adamantane-2,2′-diazirine], which produces adamantyl carbene upon photolysis, binds tightly to P450 2B4 (K_S = 3.2 μM), giving a normal substrate binding difference spectrum. Irradiation of 2-[^{3}H]adamantane diazirine at 365 nm in the presence of native, ferric P450 2B4 resulted in first-order photolysis ($t_{1/2}$ = 1.8 min). The main product was 2-[^{3}H]adamantanol, with about 6% of the radioactivity covalently bound to P450 2B4. With the ferrous carbonyl form of P450 2B4, 2-adamantanol production decreased and protein labeling increased to 12%. When ferric cyanide 2B4 was used, 2-adamantanecarbonitrile was formed in addition to 2-adamantanol. The nitrile appears to have resulted from capture of the iron-bound cyanide ligand by the carbene. The use of multiple cycles of photolysis increased the percentage of protein labeling to 76%. Photolabeling was inhibited by known 2B4 substrates and inhibitors. Also, *N*-demethylation of benzphetamine and generation of a substrate binding difference spectrum by benzphetamine were both inhibited stoichiometrically with the fraction of radiolabeled protein. The labeled protein was permanently converted to the high-spin state, as indicated by the characteristic change in the absorbance spectrum, demonstrating irreversible occupation of the substrate binding site by the adamantyl residue. Mild acid hydrolysis of radiolabeled 2B4 at the five Asp–Pro bonds generated a 2-kDa peptide which carried 78% of the radioactivity. These results are interpreted as the result of the active site carbene reacting by three competing pathways: capture of the heme sixth ligand to yield either 2-adamantanol or 2-adamantanecarbonitrile, capture of an unbound active site water molecule to yield adamantanol, and covalent attachment to a protein residue. Thus, the P450 2B4 active site appears to contain at least one unbound water molecule in addition to the heme aquo sixth ligand, even when substrate is present.

Substantial progress has been achieved in the elucidation of the general features of the catalytic mechanism of the P450 cytochromes (Dawson, 1988; Groves & Watanabe, 1988; Ortiz de Montellano, 1989). In recent years, attention has shifted to questions of the tertiary structure, particularly that of the active site. The elucidation of the crystal structures of two soluble bacterial forms, P450cam and P450BM-3, has aided this process and provided important insights (Poulos *et al.*, 1985; Ravichandran *et al.*, 1993). A mystery remains following the elucidation of the structure, however, because no catalytic groups were evident other than the heme prosthetic group. Thus, questions concerning the nature of the O–O bond lysis (homolytic or heterolytic), the role of the thiolate heme ligand in catalysis, and the source of protons needed to stabilize a hypothetical polarized peroxide transition state remain unsolved. With respect to the latter question, Jacobs *et al.* (1987) presented NMR evidence that the active site of a mammalian form, P450 11A1, contained at least one molecule of water, even when the substrate molecule (cholesterol) was bound. These authors proposed that active site water molecules might serve as the requisite source of transition-state protons. Similarly, Raag and Poulos (1991) pointed out that the crystal structure of P450cam contains a highly structured water chain that links Thr252, which is in the active site, with a distant carboxylate (Glu366) and that may serve as a proton source. They also provided evidence suggesting that a disordered water molecule may occupy the active site with some substrates. Recently, Gerber and Sligar (1992) proposed a discrete role of Asp251 as a shuttle between two proton donors, Lys178 and Arg186, and Thr252, which appears to be able to hydrogen bond to a heme-bound dioxygen molecule. In this "charge relay" system, active site water molecules might only be needed to allow proton exchange between the protein catalytic residues and the bulk solvent.

Because of the lack of a crystal structure for other forms of cytochrome P450, other approaches must be used to examine the active site structures of these enzymes. Extensive use has been made of site-directed mutagenesis (Shimizu *et al.*, 1991; Imai & Nakamura, 1991; Halpert & He, 1993) and the production of chimeric proteins (Matsunaga *et al.*, 1990; Kronbach *et al.*, 1991). However, these approaches rely heavily on analogies drawn between the homologous regions of soluble P450cam and membrane-bound mammalian P450s (Nelson & Strobel, 1989). Several groups have utilized mechanism-based inhibitors to explore the cytochrome P450 active site (Ortiz de Montellano & Reich, 1986). In most cases, turnover of suicide inhibitors by P450 generated highly reactive carbon radicals which inactivated the protein by alkylation of the heme prosthetic group. Careful analysis of the regioselectivity of the *N*-phenyl porphyrins formed with one such inhibitor has yielded a topological model of the active site on the distal side of the heme in P450 2B4[1] and other 2B-family P450s (Tuck & Ortiz de Montellano, 1992; Swanson *et al.*, 1992). Acetylenic mechanism-based inhibitors, which

† This work was partially supported by Research Grant ES03600 (to R.E.W.) from the National Institutes of Health.

* Author to whom correspondence should be addressed.
‡ University of Connecticut Health Center.
§ Present address: Department of Pathology, University of Virginia Health Sciences Center, Box 214, Charlottesville, VA 22908.
‖ Bristol-Myers Squibb Pharmaceutical Research Institute.

• Abstract published in *Advance ACS Abstracts,* January 1, 1994.

0006-2960/94/0433-807$04.50/0

generate electrophilic active site ketenes rather than carbon radicals, have been applied to the 1A, 2B, and 4A families (CaJacob *et al.*, 1988; Hopkins *et al.*, 1992; Chan *et al.*, 1993). This type of inhibitor allows the covalent modification of active site nucleophiles, not only the heme. The active site of another P450 2B isozyme has been labeled indirectly by initial degradation of the heme with cumene hydroperoxide to protein-reactive fragments (Yao *et al.*, 1993).

Another technique, photoaffinity labeling, has been applied to purified mammalian cytochromes P450 1A1 and 1A2 (Obach *et al.*, 1992; Yun *et al.*, 1992). Purified steroid-binding P450 11B1 and P450 51 have also been labeled with this approach (Ohnishi *et al.*, 1993; Wright & Honek, 1992). The only 2B-family isozyme that has been studied (2B1) was labeled in rat liver microsomes, not as a purified protein (Frey *et al.*, 1986). Photoaffinity labeling, like mechanism-based inhibition, has the advantage of providing direct information concerning the amino acid architecture of the active site.

Little information about the active site structure of the phenobarbital-inducible rabbit enzyme P450 2B4 is currently available. In our continuing study of P450 2B4 active site function (White & McCarthy, 1986) and dynamics (White *et al.*, 1986), we have undertaken the development of a photoaffinity reagent for the exploration of the active site of P450 2B4. In the course of these studies, we have found that water is the principal active site nucleophile and appears to be present in the active site in both heme-ligated and unbound states.

MATERIALS AND METHODS

General Analytical Procedures. Melting points were determined on a Thomas-Hoover melting point apparatus. Infrared spectra were recorded on a Perkin-Elmer 735 instrument as potassium bromide pellets, with the use of the 1601-cm^{-1} band of polystyrene for frequency calibration. NMR spectra were determined on a GX-270 spectrometer (JEOL Ltd., Tokyo, Japan), operating at 270 MHz for ^1H and at 68 MHz for ^{13}C. Ultraviolet spectra were measured on a Varian-Cary 219 (Varian Instruments, San Fernando, CA).

Gas chromatography (GC) was performed on a Varian 3700 chromatograph (Varian Instruments, San Fernando, CA) with a flame ionization detector (N_2 as carrier gas) and a Hewlett-Packard 3390A integrator (Hewlett-Packard Co., Palo Alto, CA). The following columns were used: column A, 3% SP2230 on Supelcoport (80/100), 2 m × 4 mm; column B, 3% Carbowax 20M on Supelcoport (80/100), 2 m × 2 mm. The internal standard technique was employed for absolute quantitation. GC–MS was performed on a Hewlett-Packard 5992 instrument (Hewlett-Packard Co., Palo Alto, CA). MS–MS was conducted on a MAT TSQ instrument (Finnigan MAT, San Jose, CA) with methane or ammonia chemical ionization.

High-pressure liquid chromatography (HPLC) was accomplished on a Perkin-Elmer series 4 pump (Perkin-Elmer Corp., Norwalk, CT) equipped with an Isco V4 variable wavelength UV detector (Isco, Inc., Lincoln, NE) and a Brownlee Spheri-5 RP-18 column (22 cm × 4.6 mm). The flow rate was always 1 mL/min. Liquid scintillation counting was performed on a Tri-Carb 4000 (Packard Instrument Co., Meriden, CT). Protein was determined using the Pierce Protein Assay (Pierce, Rockford, IL) with either bovine serum albumin or purified P450 2B4 as standard.

Cytochrome P450 concentrations were determined from absolute spectra of the ferrous carbonyl derivative. Two different procedures were used, depending on the state of the sample to be analyzed. (A) For slightly precipitated samples from experiments involving extensive handling of the enzyme, a molar absorptivity of 91 mM^{-1} cm^{-1} (determined in this laboratory) was applied to the absorbance difference (450 – 490 nm, reduced CO). (B) For optically clear solutions of cytochrome P450, a molar absorptivity of 110 mM^{-1} cm^{-1} was applied to the absolute absorbance at 451 nm (White & Coon, 1982).

Materials. Benzphetamine hydrochloride, catalase, dilauroylphosphatidylcholine, isocitric acid, isocitric dehydrogenase, metyrapone, $NADP^+$, and Tergitol NP-10 were obtained from Sigma Chemical Co. (St. Louis, MO). Amberlite XAD-2 and Coomassie Brilliant Blue R-250 were from Bio-Rad. DE52 was obtained from Whatman Ltd. (Hillsboro, OR), and sodium dithionite was from J. T. Baker Chemical Co. (Phillipsburg, NJ).

Protein Preparation. Rabbit liver cytochrome P450 2B4 ($P450_{LM2}$; official name, CYP2B4; Nelson *et al.*, 1993) was prepared by the general method outlined by Coon *et al.* (1978), with modifications (McCarthy & White, 1983). In the final electrophoretically homogeneous preparation, the ratio of the absorbance at 418 nm to that at 280 nm (R_Z number) was 1.53, and the specific heme content of the protein was 16.6 nmol of P450/mg of protein (theoretical value, 17.9 nmol of P450/mg of protein based on the enzyme molecular weight of 55 800). Rabbit liver NADPH-cytochrome P450 reductase was prepared by the general procedure of French and Coon (1979), except that DE52 was substituted for DEAE-cellulose and Tergitol NP-10 for Renex 690.

Organic Syntheses. (A) Bromoadamantanone. Adamantanone (1.50 g, 10 mmol), *N*-bromosuccinimide (1.78 g, 10 mmol), and benzoyl peroxide (0.05 g, 0.2 mmol) were allowed to reflux in chlorobenzene (25 mL) for 24 h under N_2. Removal of chlorobenzene under reduced pressure yielded a brown oil, which was dissolved in ether (50 mL) and sequentially washed with saturated sodium bisulfite, 0.1 M HCl, and saturated sodium bicarbonate (2 × 25 mL each). Preparative GC on the crude reaction mixture (column A; 150 °C for 12 min, 10 °C/min; 350 °C final temperature; collection time, 8–18 min) yielded about 1 g of white, crystalline monobromoadamantanone (mixture of at least four isomers). GC–MS analysis indicated this material was free of adamantanone and dibromoadamantanone.

(B) [^3H]Adamantanone. High specific activity catalytic tritiation was performed on the bromoadamantanone by Amersham Corp. (Chicago, IL). The crude [^{3}H]adamantanone received from Amersham was found to be 77% radiochemically pure by thin-layer chromatography on silica gel G plates with chloroform as solvent (R_f = 0.58), which was confirmed by reverse-phase HPLC. Radiochemically pure [^{3}H]adamantanone was obtained by preparative TLC.

(C) [^3H]Spiro[adamantane-2,2′-diazirine]. [^{3}H]Spiro-[adamantane-2,2′-diazirine] was synthesized by the method of Bayley and Knowles (1980). 2-[^{3}H]Adamantanone (113 mg, 0.75 mmol, 1.22 mCi) was converted to the intermediate diaziridine (radiochemical yield, 760 μCi, 62%), which was carried to the next step without further purification. The product [^{3}H]diazirine (224 μmol, 30% yield) was stored as a

[1] Abbreviations: P450 2B4, phenobarbital-inducible rabbit liver microsomal cytochrome P450 (CYP2B4; Nelson *et al.*, 1993); DLPC, dilauroylphosphatidylcholine; DMPC, dimyristoylphosphatidylcholine; K_S, spectrally determined apparent dissociation constant; SDS–PAGE, sodium dodecyl sulfate–polyacrylamide gel electrophoresis; TFA, trifluoroacetic acid.

50 mM solution in methanol at −20 °C until use. The UV spectrum was in excellent agreement with that observed by Bayley and Knowles (1980), and the concentration of the diazirine solution was determined by A_{372} ($\epsilon = 245\ M^{-1}\ cm^{-1}$). The product was shown to be 99% radiochemically pure by thin-layer chromatography and by HPLC (65% MeCN:35% H_2O; detection at 220 and 376 nm). The specific activity of the diazirine was 1.86 mCi/mmol (4130 dpm/nmol).

A parallel synthesis of nonradiolabeled diazirine gave an overall yield of 46% from adamantanone. Proton NMR and IR spectra were consistent with those reported by Bayley and Knowles (1980). The ^{13}C NMR spectrum consisted of the expected five signals (chemical shift (relative intensity)): δ ($CDCl_3$) 27.5 (0.49), 34.4 (0.35), 34.8 (0.11), 35.0 (1.00), 36.7 (0.26) ppm. No peak assignments were made.

(D) 2-[^3H]Adamantanecarbonitrile. 2-Adamantanecarbonitrile was synthesized according to the method of Oldenziel *et al.* (1977). 2-[^{3}H]Adamantanone (1.50 g, 10 mmol, 40.8 μCi) and tosylmethyl isocyanide (2.50 g, 13 mmol; Aldrich Chemical Co.) were converted to 2-[^{3}H]adamantanecarbonitrile (1.52 g, 9.4 mmol, 94% yield) with a melting range of 174–180 °C (lit. 160–180 °C) and a specific activity of 8.33 dpm/nmol. GC analysis (column B, 130 °C) indicated that the product was 99.8% pure. The infrared spectrum exhibited a peak at 2240 cm^{-1} confirming the presence of a nitrile function. Positive ion chemical ionization mass spectrometry with ammonia as reagent gas showed a strong molecular ion at m/z 179, expected for $(M + NH_4)^+$. The negative ion mass spectrum showed the expected deprotonated molecular ion at m/z 160 for $(M - H)^-$. The ^{1}H NMR spectrum was as follows: δ ($CDCl_3$) 1.73 (unresolved doublet, 2 H), 1.77 (unresolved doublet, 4 H), 1.87 (singlet, 1 H), 1.91–1.94 (unresolved doublet, 3 H), 2.13 (singlet, 1 H), 2.17 (singlet, 3 H, CH–CH–CN), 2.90 ppm (singlet, 1 H, CH–CN). The ^{13}C NMR spectrum was as follows: δ (relative intensity; $CDCl_3$) 26.78 (0.55), 26.92 (0.49), 30.44 (0.96), 33.11 (0.94), 36.66 (1.00), 36.74 (0.66), 37.03 (0.38), 122.21 ppm (0.10).

(E) 2-[^3H]Adamantanecarboxylic Acid. Radiolabeled 2-adamantanecarboxylic acid was synthesized by the method of Stetter and Tilmanns (1972). 2-[^{3}H]Adamantanecarbonitrile (0.50 g, 3.1 mmol, 7.4 μCi) was hydrolyzed in refluxing 48% hydrobromic acid to yield 2-[^{3}H]adamantanecarboxylic acid (0.47 g 2.6 mmol, 84%) as white needles with a melting point of 143–144 °C (lit. 143–144 °C) and a specific activity of 5.50 dpm/nmol. Infrared analysis indicated the presence of carboxylic acid by the O—H stretch at 3025 cm^{-1} and the C=O stretch at 1701 cm^{-1}. The positive ion chemical ionization mass spectrum with ammonia as reagent gas showed a strong molecular ion at m/z 198, expected for $(M + NH_4)^+$. The ^{1}H NMR spectrum was as follows: δ ($CDCl_3$) 1.6–2.0 (multiplet, 12 H), 2.36 (singlet, 2 H, CH–CH–COOH), 2.67 (singlet, 1 H, CH–COOH), 10–11 ppm (very broad, 1 H, COOH). The ^{13}C NMR spectrum was as follows: δ (relative intensity; $CDCl_3$) 27.38 (0.72), 29.37 (0.57), 33.55 (0.82), 37.32 (0.49), 38.07 (1.00), 49.41 (0.38, CH–COOH), 180.93 ppm (0.19, COOH).

(F) 2-[^3H]Adamantanol. 2-[^{3}H]Adamantanol was prepared by photolysis of [^{3}H]spiro[adamantane-2,3′-diazirine] (450 nmol, 1.08 μCi) in water for 1 h at 365 nm. Reaction progress was monitored by disappearance of the characteristic UV spectrum and by HPLC (70% CH_3CN: 30% H_2O, 376 nm). The product (1.02 μCi, 94% radiochemical yield) was identified as 2-adamantanol and found to be pure by GC by comparison to nonradioactive standard. The radiochemical purity was 98% by HPLC.

Adamantane Diazirine Binding to P450 2B4. The affinity of adamantane diazirine for P450 2B4 was measured by monitoring the spectral change accompanying substrate binding (Jefcoate, 1978). The reconstituted enzyme/lipid system used in the spectral titrations contained cytochrome P450 2B4 (20 nmol), DLPC (varying from 100 to 500 μg/mL), potassium phosphate (100 μmol, pH 7.4), and 20% glycerol in a final volume of 2 mL. The enzyme solution was divided between the sample and reference cuvettes. The apparent dissociation constant (K_S) of the diazirine at each lipid concentration was determined with double-reciprocal plots. Substrate-depletion effects due to diazirine binding to the enzyme were corrected by a computer algorithm that employed successive approximations of ΔA_{max} to estimate bound diazirine at each total diazirine concentration point in an iterative procedure which converged on a constant value of K_S. Diazirine concentration points requiring more than 80% correction were not used in the analysis.

Photoaffinity Labeling. The photochemical reactor consisted of a Spectronics Model B-100 UV lamp (Fisher Scientific, Springfield, NJ) and a refrigerated sample holder mounted on a lab jack to allow sample height adjustment. The focus of the lamp was centered on the sample compartment at a lamp-to-sample distance of 1 cm, giving an estimated UV flux at the sample of 10 W/cm^2. The enzyme solution to be photolyzed consisted of P450 2B4 (10 μM), DLPC (300 μg/mL), potassium phosphate (100 mM, pH 7.4), and 20% glycerol in a final volume of 1 mL. In some experiments, a competitive inhibitor (*i.e.*, benzphetamine, metyrapone, or adamantane) was added at this point. The enzyme solution was placed in a septum-sealed 12 × 75 mm glass test tube. The solution was deoxygenated as previously described (White & Coon, 1982). For photolysis of the ferrous carbonyl form, carbon monoxide was bubbled through the solution for 1 min, and then sodium dithionite (250 nmol) was added as a 50 mM solution in 50 mM sodium borate buffer, pH 9.1. The sample was allowed to stand for 5 min to allow complete reduction of the cytochrome. For photolysis of the ferric cyanide form, 70 mM sodium cyanide was included in the photolysis buffer, and the additions of carbon monoxide and dithionite were omitted. A solution of [^{3}H]adamantane diazirine (10 mM in methanol) was added to yield a final diazirine concentration of 5 μM. In single-cycle experiments, the diazirine/enzyme solution was photolyzed for 20 min (10 half-lives) at 15 °C. In multiple-cycle experiments, the solution was photolyzed for 3 min (1.5 half-lives); then another aliquot of diazirine was added, and the sample was photolyzed for an additional 3 min. The addition of fresh diazirine every 3 min continued for a total of 10–20 cycles. After the final aliquot of diazirine, the solution was photolyzed for 20 min. Multiple-cycle samples to be used for determination of benzphetamine binding or enzymatic activity, spectroscopy, or TFA hydrolysis were dialyzed overnight against 4 L of buffer containing 100 mM potassium phosphate, pH 7.4, 20% glycerol, and Amberlite XAD-2 (10 g/L) to remove methanol and 2-adamantanol. During the aerobic dialysis period, the reduced (ferrous) protein reverted to the ferric state.

Fractionation of Photolysis Reaction Mixtures. Method I. This procedure was employed when only the degree of label incorporation into apoprotein was to be determined. Following photolysis, apoprotein was precipitated by the addition of an equal volume of 1.2 M HCl in butanone (Wagner *et al.*, 1981), and the pellet was further extracted with acidic butanone (4 × 1 mL). The butanone extracts contained the organic products, lipid, and heme, while the pellet consisted

solely of apoprotein. Apoprotein pellets were resuspended in 1 mL of 10% sodium dodecyl sulfate containing 0.1 M NaOH by heating at 100 °C for 5 min. The base was neutralized with 20 μL of glacial acetic acid prior to scintillation counting to prevent chemiluminescence. In control samples containing either 2-[^{3}H]adamantanol or [^{14}C]DMPC as tracer, no radioactivity was associated with the protein pellet, demonstrating efficient extraction of organics and lipid from the protein. Assay of protein content before and after the acidic butanone step indicated that 98% of the protein was precipitated.

Method II. This procedure was employed to separate photolysis reaction mixtures into four fractions: organic, phospholipid, heme, and protein. Radiolabel could then be quantitated in each fraction. Following photolysis, the protein was precipitated with an equal volume of 17.5% perchloric acid (PCA), and the resulting pellet and supernatant were extracted with ether (4 × 1 mL) to isolate organic reaction products. The pellet was washed with water (2 × 1 mL) to remove residual PCA and extracted with neutral acetone (4 × 1 mL) to obtain a lipid fraction. The heme was removed from the precipitated protein with acidic butanone (4 × 1 mL). The efficiencies of extraction of organics and lipid were measured with radiolabeled 2-[^{3}H]adamantanol and [^{14}C]-DMPC. All of the 2-adamantanol activity was associated with the ether extracts, while the lipid activity was found entirely in the acetone extracts. The recovery of protein in the pellet was 95%.

Analysis of Organic Products of Photolysis. Identification of the organic photolytic products was performed by HPLC of an aliquot of the ether extract (50 μL) from fractionation method II. Analysis of extracts containing 2-adamantanecarbonitrile used an initial mobile phase consisting of methanol:water (50:50) for 8 min, followed by an increase to 100% methanol over a period of 3 min. Analysis of extracts expected to contain 2-adamantanecarboxylic acid used methanol:water (45:55, isocratic) containing 0.03% acetic acid. Fractions (1 mL) were collected and analyzed for radioactivity. The retention times of the products were determined by reference to radiolabeled standards synthesized as above. In addition, the HPLC retention times for the 2-adamantanol and 2-adamantanecarbonitrile standards were confirmed by GC analysis of the HPLC fractions (column B, 130 °C).

Substrate-Binding Capacity of Labeled Protein. The protein was photolyzed (20 cycles) in the presence of adamantane diazirine as described above, except that the amounts of all reagents were doubled to give a final volume of 2 mL. Following dialysis, the entire enzyme solution was divided between two cuvettes and spectrally titrated as described above, except that benzphetamine (stock concentration, 100 mM in water) was used rather than adamantane diazirine. At the end of the titration, the reference cuvette was replaced with one containing buffer and the total P450 concentration was determined. Observed benzphetamine-induced absorbance differences were corrected for concentration changes introduced by the dialysis step.

Enzymatic Activity of Labeled Protein. The benzphetamine *N*-demethylase activity of P450 2B4 was assayed in a reconstituted system consisting of P450 2B4 (0.3 nmol), NADPH-cytochrome P450 reductase (1 nmol), DLPC (100 μg added as a sonicated suspension in water), potassium phosphate (100 μmol, pH 7.4), benzphetamine (1 μmol), catalase (3000 units), and a NADPH-generating system, in a total volume of 1 mL. The NADPH-generating system consisted of isocitric dehydrogenase (0.3 unit), $NADP^+$ (400 nmol), isocitric acid (5 μmol), and $MgCl_2$ (10 μmol). Under these conditions, P450 2B4 was the rate-limiting component. Reactions were initiated by the addition of $NADP^+$ and allowed to proceed at 25 °C for 2 min, and the reaction mixtures were assayed for formaldehyde by the method of Nash (1953) as modified by Cochin and Axelrod (1959). Because some loss of activity (9–11%) occurred during the extensive handling of the enzyme in this experiment, photoexposed controls were carried through the entire procedure, but with diazirine omitted in the photolysis step. Activities of photolabeled enzyme samples were compared to the appropriate controls.

Trifluoroacetic Acid Hydrolysis of Photolabeled Protein. Hydrolytic digestion of labeled P450 2B4 at aspartic acid–proline bonds was accomplished in 0.1% trifluoroacetic acid (TFA) by a modification of the method of Tarr *et al.* (1983). The radiolabeled protein was incubated with 1 mM dithiothreitol (DTT) for 30 min at 60 °C and then was precipitated with an equal volume of 17.5% PCA and washed with acetone (2 × 1 mL) to remove lipid. The protein pellet was washed with water (3 × 1 mL) to remove residual PCA, dissolved in 0.1% TFA at a concentration of 5 μM, and heated at 100 °C for 1 h. The hydrolysate was lyophilized and then analyzed by SDS-PAGE. Molecular masses were calibrated with myoglobin peptides (MW-SDS-17, Sigma Chemical Co., St. Louis, MO) that ranged from 2.5 to 17 kDa. Analysis of radiolabel incorporation was accomplished by digestion of the gel slices in a 90% solution of NCS tissue solubilizer at 50 °C for 2 h, followed by scintillation counting.

RESULTS

Binding of Adamantane Diazirine to P450 2B4. The successive addition of [^{3}H]adamantane diazirine to a solution of P450 2B4 induced a series of type I binding spectra of increasing magnitude (Figure 1). A double-reciprocal plot of the magnitude of these spectra as a function of free substrate concentration indicated that the K_S of the P450/diazirine complex was 3.2 μM (Figure 1, inset). This experiment was conducted at several DLPC concentrations in order to optimize the binding affinity of the diazirine. The K_S varied from a maximum of 10 μM at 100 μg/mL to a minimum of 3.2 μM at 300 μg/mL. Above 300 μg/mL, the K_S increased.

Photolysis of P450 2B4/Diazirine Complex. The photolysis procedure was optimized for maximum incorporation efficiency and active site selectivity. The UV lamp selected allowed short photolysis times, and spectral output was confined to wavelengths between 310 and 380 nm, minimizing possible photolytic damage to the P450, which absorbs strongly below 300 and above 400 nm. In addition, the spectral maximum of the lamp (365 nm) was near the absorption maximum of the diazirine (372 nm).

The time course of photolysis of the P450/diazirine complex could be monitored by the reversal of the diazirine binding spectrum, as illustrated in Figure 2. The decay kinetics were first order, with a half-life of 1.8 min for the disappearance of the binding spectrum. The photolysis of the diazirine alone under the same conditions had a half-life of 0.8 min, less than half that of the P450/diazirine complex. The slower photolysis rate of the P450/diazirine complex is attributable to an inner-filter effect of the heme chromophore (see Discussion).

In the initial exploratory experiments with protein labeling, incorporation of the photolabel into protein was found to increase according to the binding affinity of the diazirine at the various DLPC concentrations. The highest labeling efficiency occurred at the DLPC concentration producing the lowest K_S (*i.e.*, 300 μg/mL), as expected if the labeling were

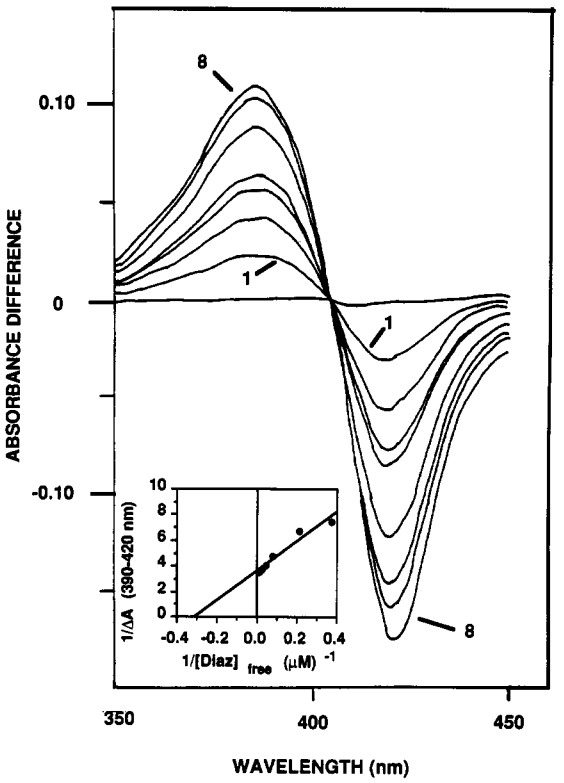

FIGURE 1: Difference spectra of adamantane diazirine binding to P450 2B4. The concentrations of P450 and DLPC were 10 μM and 300 μg/mL, respectively. Curves 1–8 represent total diazirine concentrations of 2.5, 5.0, 7.5, 10, 20, 30, 50, and 100 μM. Inset: Benesi–Hildebrand analysis of adamantane diazirine binding spectra.

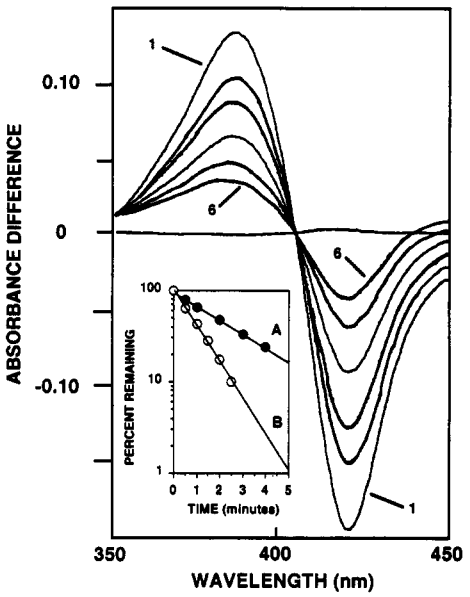

FIGURE 2: Reversal of diazirine-induced binding spectra during photolysis. The concentrations of P450 and diazirine were 10 μM. Spectra 1–6 represent irradiation times of 0, 0.5, 1, 2, 3, and 4 min. Inset: First-order kinetic analysis of photolysis time course. Curve A depicts the decay of the diazirine-induced binding spectrum ($t_{1/2}$ = 1.8 min). Curve B illustrates the decay of diazirine when photolyzed in the absence of P450 ($t_{1/2}$ = 0.8 min). The concentration of diazirine was monitored at 376 nm.

active site directed. Therefore, this concentration was chosen for all subsequent photolabeling studies. Substoichiometric quantities of diazirine compared to P450 2B4 (5 and 10 μM, respectively) were used in the photolabeling procedure (see Discussion). Thus, multiple cycles of replenishment of diazirine and photolysis were necessary to achieve reasonable

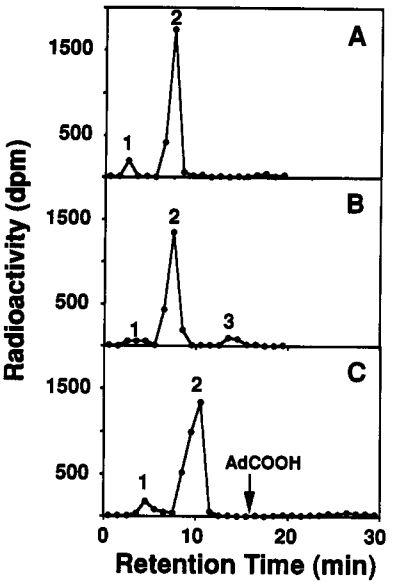

FIGURE 3: HPLC chromatogram of organic products of photolysis. Conditions were as described under Materials and Methods. Panel A: Products from photolabeling of native ferric P450 2B4. Peak 1 represents adamantyl phosphate, as described under Results, while Peak 2 represents 2-adamantanol. Panel B: Products from photolabeling of ferric cyanide P450 2B4. Peak 1 represents adamantyl phosphate; peak 2, 2-adamantanol; and peak 3, 2-adamantanecarbonitrile. Panel C: Products from photolabeling of ferrous carbonyl P450 2B4. Peak 1represents adamantyl phosphate, while peak 2 represents 2-adamantanol. The arrow indicates the retention time of 2-adamantanecarboxylic acid, which was not present.

Table 1: Radioactive Product Yield after Photolysis under Various Conditions (% of Total Radioactivity)[a,b]

	conditions of photolysis			
radioactive product	Fe^{3+}, N_2	Fe^{3+}, CN^-	Fe^{2+}, N_2	Fe^{2+}, CO
adamantanol	79.6	68.5	72.1	68.2
adamantyl phosphate	7.0	7.5	10.4	8.7
dehydroadamantane	ND[c]	ND	ND	2.5
admantanecarbonitrile	ND	6.2	*d*	*d*
adamantanecarboxylate	*d*	*d*	ND	ND
DLPC	6.6	7.0	9.3	7.5
heme	1.1	1.2	1.0	1.2
apoprotein	5.8	9.6	7.1	12.0

[a] Single-cycle photolysis. [b] Data are presented as the average of duplicates. Individual values differed from the means by less than 3% (relative). [c] ND = Product not detected. [d] Product not determined.

fractions of protein labeling. SDS–PAGE of the photolabeled protein demonstrated that the radioactivity migrated with the protein, indicating that the label was not dissociable under these severely denaturing conditions. We infer that the radiolabel must have been covalently attached to P450 2B4.

Organic Products of Photolysis. The main volatile organic product obtained by photolysis of the diazirine under the standard protein labeling conditions was 2-adamantanol (Figure 3A), representing approximately 80% yield from added diazirine under anaerobic ferric photolysis conditions (Table 1). The alcohol was produced under anaerobic as well as aerobic conditions, showing that production of 2-adamantanol represents carbene capture of water rather than of molecular oxygen. The implications of this high degree of 2-adamantanol production for conclusions about the active site environment will be discussed in the next section. In addition, a more polar product was observed (7% yield), with a retention time of approximately 2.5 min, which was most likely 2-adamantyl phosphate. A third organic product observed under nonenzymatic conditions or when the ferrous carbonyl derivative of

P450 was photolabeled had a retention time similar to that of adamantane and was most likely dehydroadamantane (*i.e.*, the rearrangement product of adamantane carbene), as described by Bayley (1983).

Ligand Capture. Because the production of 2-adamantanol during photolabeling of P450 2B4 was unexpectedly high, this process was examined in more detail. The fraction of adamantane diazirine which was not bound in the active site at the beginning of photolysis can be calculated to be 33% (10 μM enzyme, 5 μM diazirine, K_S = 3.2 μM). After one photolytic half-life, the free fraction should decrease slightly to 28%. Since the yield of 2-adamantanol under ferric conditions was nearly 80%, rather than approximately 30%, an appreciable yield of 2-adamantanol appeared to have resulted from carbene capture of a water molecule *within the active site*. With ferrous P450 2B4, the yield of 2-adamantanol decreased somewhat. Since the ferrous form lacks a sixth ligand (White & Coon, 1982), this suggested that at least some of the water captured by the carbene with the ferric form might have been the heme water ligand.

To address the question of capture of the heme sixth ligand by the carbene, experiments were conducted in which the ligand was either cyanide or carbon monoxide. The results are shown in Table 1. In the presence of cyanide, the percent incorporation of label into protein under ferric conditions increased from 5.8% to 9.6%. In the presence of carbon monoxide, the incorporation under ferrous conditions more than doubled to 12.0%. HPLC analysis of the organic fraction (Figure 3B) under ferric cyanide conditions indicated that a significant amount of diazirine was converted to 2-adamantanecarbonitrile, which provided direct chemical evidence for ligand capture. However, as can be seen in Figure 3C, the carbon monoxide ligand was not captured to yield the potential capture product 2-adamantanecarboxylic acid.

In addition to demonstrating that a portion of the 2-adamantanol product arose from capture of the heme sixth ligand, these experiments also provided a method for increasing the efficiency of covalent radiolabeling of the protein. Carrying out photolysis in the ferrous state under carbon monoxide, so that the sixth ligand was not a capturable one, more than doubled the fraction of protein labeled in each cycle. The combined use of multiple photolytic cycles and ligand replacement allowed large extents of protein labeling. Thus, whereas the single-cycle photolysis of the ferric form yielded only 6% labeled protein, 20-cycle photolysis of the ferric cyanide and ferrous carbonyl forms yielded 54% and 76% labeled protein, respectively. These procedures were used in subsequent studies to maximize the production of labeled protein.

Competitive Inhibition of Photolabeling by Substrate Analogs. Three structurally diverse compounds, benzphetamine, adamantane, and metyrapone, known substrates or inhibitors of P450 2B4, were used as competitive inhibitors of protein photolabeling by adamantane diazirine. As seen in Table 2, the incorporation of photolabel into protein was inhibited by 87% in the presence of 100 μM adamantane, indicating that protein labeling occurred principally in the active site. Substantial inhibition was also observed with benzphetamine and metyrapone.

Inhibition of Enzymatic Activity. Covalent modification of active site residues involved in either substrate binding or catalysis should interfere with the enzymatic activity of photolabeled P450 2B4, such as the *N*-demethylation of benzphetamine. The relative enzymatic activity of P450 labeled in the presence of cyanide compared to that of

Table 2: Inhibition of Photolabeling of P450 2B4 by Known Substrates and Inhibitors

compound	concn (μM)	K_S (μM)[a]	cycles of photolysis	inhibition[b,c]
benzphetamine	2000	100	10	56%
			1	76%
adamantane	100	2	10	85%
			1	87%
metyrapone	100	2	10	66%

[a] Determined by spectral titration as described under Materials and Methods. [b] Inhibition = {1 – (nmol of P450 labeled in sample/nmol of P450 labeled in control)} × 100%. [c] Samples were treated in duplicate, and results did not vary by more than 5%.

Table 3: *N*-Demethylation of Benzphetamine by P450 2B4 Photolabeled in the Presence of Sodium Cyanide or Carbon Monoxide[a]

enzyme state	rel rate[b]	fraction of unlabeled protein[c]
native[d]	1.09 ± 0.02[e]	0.00
photoexposed as ferric cyanide[f]	1.00 ± 0.01	0.00
photolabeled as ferric cyanide	0.47 ± 0.01	0.46
native[g]	1.11 ± 0.01[h]	1.00
photoexposed as ferrous carbonyl[f]	1.00 ± 0.01	1.00
photolabeled as ferrous carbonyl	0.36 ± 0.01	0.24

[a] Twenty photolytic cycles. [b] Average of 10 replicate determinations ± standard error of the mean. [c] Based on radiolabel incorporation. Fraction unlabeled = 1 – (mol of radiolabel/mol of P450). [d] Enzyme not photolyzed; neither diazirine nor sodium cyanide added. [e] The absolute rate of native enzyme-catalyzed demethylation was 14 mol/mol of P450/min. [f] Carried through photolysis procedure, but with diazirine omitted. [g] Enzyme not photolyzed; neither diazirine nor carbon monoxide added. [h] The absolute rate of native enzyme-catalyzed demethylation was 15.1 mol/mol, of P450/min.

photoexposed control protein was 0.47 (Table 3), in excellent agreement with the fraction of unlabeled protein (0.46). In other words, photolabeling completely abolished the ability of the labeled fraction of P450 2B4 to *N*-demethylate benzphetamine, while the activity of the unmodified P450 molecules in the sample remained intact. When the photolysis was carried out in the presence of carbon monoxide, the relative enzymatic activity of photolabeled protein was 0.36 (Table 3), in reasonable agreement with the fraction of unlabeled protein remaining after photolabeling (0.24).

Permanently Induced Difference Spectrum. Permanent occupation of the active site of P450 2B4 by a covalently attached photolabel should give rise to a nonreversible spectral change, similar to that induced by substrate binding. The spectra of the protein labeled in the ferrous carbonyl form are seen in Figure 4A. After dialysis, which converted the ferrous to the ferric form, the spectrum of the photolabeled protein resembled that of the native ferric enzyme. Close inspection, however, reveals an inflection at 390 nm, corresponding to the absorbance maximum for the high-spin, substrate-bound form of the enzyme. When the enzyme was reconverted to the ferrous carbonyl form, the spectrum of the labeled protein showed a small amount of denaturation to cytochrome P420 (*ca.* 13%) as a result of dialysis. Similar spectra of the protein labeled as the ferric cyanide derivative are shown in Figure 4B. In this case, there was no conversion to P-420, because of the greater stability of the ferric form.

The spectra of the photolabeled protein and the native P450 were digitized to permit manual generation of a difference spectrum (Figure 5). The permanently induced difference spectrum clearly resembled the binding difference spectra obtained by addition of benzphetamine, a classic type I

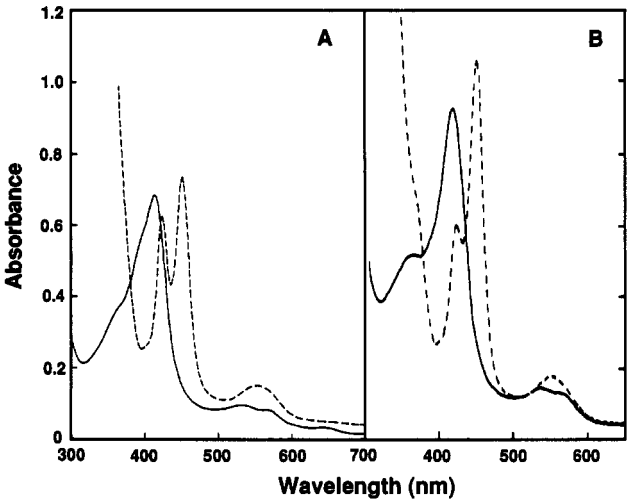

FIGURE 4: Ultraviolet–visible spectra of photolabeled P450 2B4. Protein was labeled for 20 photolytic cycles as the ferrous carbonyl derivative (panel A) or the ferric cyanide derivative (panel B) and dialyzed, as described under Results. The spectra were obtained immediately following dialysis. In panel A, note the asymmetry at 390 nm in the ferric spectrum, which is not clearly visible in panel B. The ferrous carbonyl spectrum in panel A indicates a small degree of denaturation to P-420, which is absent in panel B.

substrate, to native P450 with a peak at 390 nm, an isosbestic point at 405 nm, and a trough at 420 nm. Thus, photolabeling of P450 2B4 induced a binding spectrum in the enzyme that was not reversible by dialysis, indicative of the presence of an irreversibly bound substrate in the active site.

By applying the known difference extinction coefficient of 0.126 μM^{-1} cm^{-1} (White & McCarthy, 1986) to the 390–420-nm absorbance difference, one can calculate that the concentration of high-spin P450 in the sample increased from 0.8 to 7.4 μM. Correction for the small high-spin component of the 24% of unmodified protein present gave 7.2 μM as the concentration of high-spin P450 in the modified fraction. Since the concentration of radiolabeled P450 in the sample was 7.6 μM, we conclude that the modified protein was 95% in the high-spin state. The near equivalence of the high-spin content (7.2 μM) and the radioactivity content (7.6 μM) served as an independent verification of the specificity of the photoaffinity labeling process. At least 95% of the radioactive adamantyl residues must have been associated with the active site to be able to produce the active site specific spin-state change.

Inhibition of Substrate Binding in Photolabeled Protein. Permanent occupation of the active site of P450 2B4 by a covalently attached adamantyl residue should also interfere with the binding of substrates. To determine whether substrate binding was altered in the labeled protein, the affinity of benzphetamine for the enzyme was measured by titration of the type I binding difference spectrum. The series of type I binding spectra obtained by successive addition of benzphetamine to control protein are seen in Figure 6A. In contrast, the titration of equal amounts of benzphetamine to the photolabeled proteins resulted in binding spectra of smaller magnitude (Figure 6B,C). Double-reciprocal plots of the substrate concentration versus the absorbance difference of these binding spectra confirmed that the maximum absorbance difference (ΔA_{max}) was smaller in the photolabeled proteins than in the control (Table 4). However, the K_S values obtained from the x-intercepts were essentially identical, demonstrating similar benzphetamine affinities for the proteins labeled to different extents. The relative absorbance maxima obtained in the control and labeled forms of P450 closely paralleled the fractions of unlabeled protein. This stoichiometric loss of

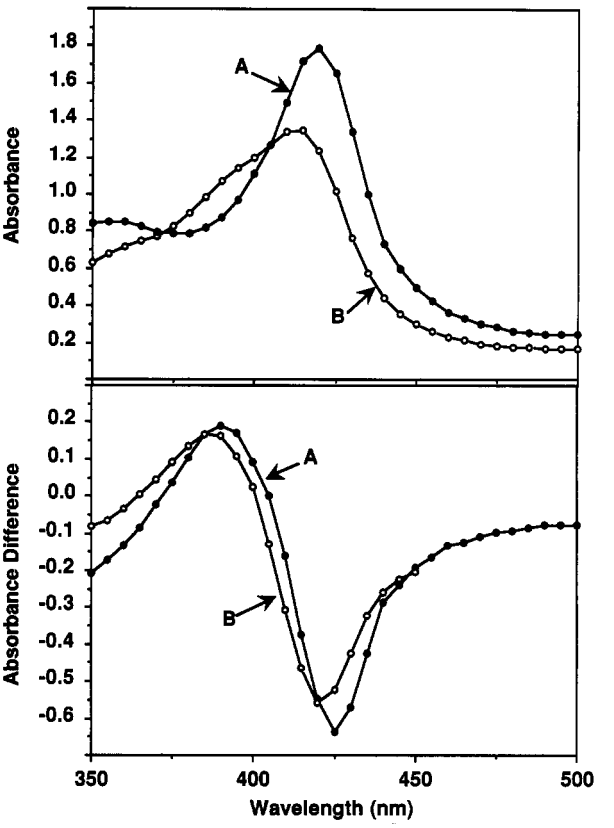

FIGURE 5: Digitized ultraviolet–visible spectra of photolabeled and native P450 2B4. Top panel: Absolute spectra generated by plotting the observed protein absorbance as a function of wavelength at 5-nm intervals for the native (curve A) and the photolabeled protein (curve B). Protein was photolabeled as the ferrous carbonyl derivative as described under Results. However, because of air oxidation during overnight dialysis, both protein samples were in the ferric state during spectroscopy. Bottom panel: Permanent induced difference spectrum of photolabeled protein. Curve A is the difference spectrum generated by manual subtraction of the photolabeled protein spectrum from that of native P450. Curve B is the difference spectrum of benzphetamine-bound compared to native protein. The photolabeled and benzphetamine-bound absolute spectra were corrected for concentration and 405-nm offset prior to generation of the difference spectra.

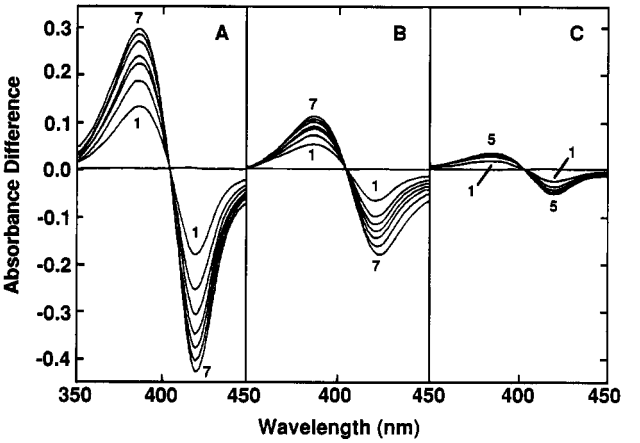

FIGURE 6: Difference spectra of benzphetamine binding to photolabeled P450 2B4. Protein was photolabeled and dialyzed as described under Results. Benzphetamine was added to yield final concentrations of 50, 100, 150, 200, 300, 500, and 1000 μM for each set of titrations. Panel A represents substrate addition to photoexposed protein control. Panels B and C represent addition of substrate to protein labeled as the ferric cyanide and ferrous carbonyl derivatives, respectively.

substrate binding capacity with photolabeling may be explained by the presence of two populations of P450 in the photolabeled

Table 4: Benzphetamine Binding to P450 2B4 Photolabeled in the Presence of Sodium Cyanide or Carbon Monoxide[a]

enzyme state	K_S (μM)[b]	rel ΔA_{max}[b]	fraction of unlabeled protein[c]
native	79	1.10	1.00
photoexposed as ferric cyanide[d]	92	1.00	1.00
photolabeled as ferric cyanide	84	0.43	0.44
photolabeled as ferrous carbonyl	92	0.21	0.24

[a] Twenty photolytic cycles. [b] Determined from double-reciprocal plots. The absolute value of ΔA_{max} for native enzyme was 0.674. [c] Based on radiolabel incorporation. Fraction unlabeled = 1 – (mol of radiolabel/mol of P450). [d] Carried through photolysis procedure, but with diazirine omitted.

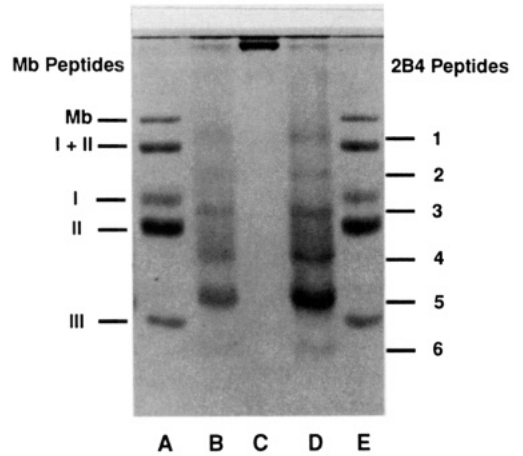

FIGURE 7: SDS–PAGE of TFA peptides from P450 2B4. Gel conditions were as described under Materials and Methods. Lane C contained purified P450 2B4 standard (0.125 nmol). Lanes B and D contained the TFA peptides. Lanes A and E contained 10 μg of a myoglobin fragment standard mixture containing peptides at 17.0, 14.4, 8.2, 6.2, and 2.5 kDa. For the P450 TFA peptides, the apparent molecular masses (% of total radiolabel) were 1, 15 kDa (0.5%); 2, 10 kDa, (0%); 3, 7 kDa (0%); 4, 5 kDa (0%); 5, 3 kDa (18.3%); and 6, 2 kDa (78.1%).

samples. The unlabeled fraction of P450 was able to bind benzphetamine with its normal affinity, giving rise to a K_S similar to that of control protein and a ΔA_{max} proportional to its concentration. On the other hand, the labeled protein fraction completely lost the ability to bind benzphetamine and generated no binding spectrum. The net result was the observed proportional decrease in the maximal magnitude of the binding difference spectrum (ΔA_{max}) while similar binding affinities were maintained.

Peptide Mapping. Peptide mapping of labeled P450 2B4 was used to establish the approximate position of the covalently bound radiolabel in the protein amino acid sequence. Hydrolysis of P450 2B4 with dilute TFA has been shown to cleave the protein primarily at aspartic acid–proline peptide bonds, leading to six peptides due to the five aspartic acid–proline peptide bonds (Tarr *et al.*, 1983). TFA-catalyzed cleavage of labeled P450 2B4 and separation of peptides by SDS–PAGE resulted in almost complete disappearance of the intact protein band and generation of six peptides of approximately the size expected from the known primary structure (Figure 7). As compiled in Figure 7, the majority of the radioactivity (78.1%) was found in the smallest peptide, with an apparent molecular mass of about 2 kDa. The smallest TFA peptide contains 21 amino acids with the sequence ^{258}PSNPRDFIDVYLLRMEKDKSD (Tarr *et al.*, 1983), but we have not yet identified the particular amino acid residue(s) that were modified. A second band, which contained most of the remainder of the label (18.3%), had an apparent molecular mass of about 3 kDa.

DISCUSSION

Selection of 2-Adamantane Diazirine. A diazirine is a logical choice for a photoaffinity reagent because photolysis of diazirines yields carbenes, which are potent electrophiles capable of capturing active site nucleophiles as well as inserting into C–C and C–H bonds, and the active site of P450 2B4 is expected to have many hydrophobic amino acid residues. Although the extinction coefficient of the diazirine is modest (ϵ = 245 M^{-1} cm^{-1}, 372 nm), a high quantum yield results in an appreciable rate of photolysis. Data on the lifetime of photogenerated carbenes is scarce, but comparison to other carbenes suggests that adamantyl carbene should have an extremely short half-life in the range of 20 ps to 2 μs, depending of the environment and the state of the carbene (Bayley, 1983). Thus, it is unlikely to move far from its point of origin. 2-Adamantane diazirine was expected to have a high affinity for the P450 2B4 active site, since it is a close structural analog of adamantane and 2-adamantanone, which have K_S values of 2 and 65 μM, respectively, for this isozyme (White *et al.*, 1984). Furthermore, the tricyclic structure precludes olefin formation, a process which occurs readily with alkyl diazirines possessing an α-hydrogen (*e.g.*, photolysis of cyclohexyldiazirine produces 97% cyclohexene).

Photolysis of Protein-Bound Adamantane Diazirine. The rate of photolysis of adamantane diazirine observed in the presence of P450 was significantly slower than in its absence. This phenomenon may be explained on the basis of the inner-filter effect resulting from UV absorption by P450 2B4 in the absorption region of the diazirine. One may show that the relative rate of the photolysis of diazirine in the presence and absence of an inner filter is given by

$$\frac{(d[D]/dt)_{\text{inner filter}}}{(d[D]/dt)_{\text{control}}} = 10^{-\epsilon c l}$$

where ϵ is the molar absorptivity of the inner-filter compound, c is its concentration, and l is the path length of the beam through the sample. According to this equation, the relative rate of diazirine photolysis under our photolysis conditions ([P450] = 10 μM; $\epsilon \approx 0.04$ μM^{-1} cm^{-1}) should be less than half (0.4) of that observed in the absence of protein, in excellent agreement with the observed value of 0.44, showing that the slower rate with P450 present is due solely to the heme inner-filter effect.

Photocarbenes generated in the active site (Figure 8A) should be extremely electrophilic and could have labeled any active site amino acid residue, with a hypothetical leucine adduct shown in Figure 8B. The carbene also had the capacity to incorporate into phospholipid, heme, or components of the aqueous buffer. Covalent modification of the protein did occur and accounted for as much as 12% of the single-cycle carbene reaction products depending on the experimental conditions. Heme labeling could be predicted on the basis of the presence of the electron-rich π system. Surprisingly, however, only about 1% of the photolabel was found attached to the heme. This was in sharp contrast to earlier work involving generation in the active site of highly reactive species such as carbon radicals (Grab *et al.*, 1988; Swanson *et al.*, 1992; Tuck & Ortiz de Montellano, 1992), benzyne (Ortiz de Montellano *et al.*, 1984), and cyclobutadiene (Stearns & Ortiz de Montellano, 1985) that reacted extensively with the heme.

Optimization of Photolabeling of Adamantane Diazirine to P450 2B4. The ratio of diazirine to P450 was chosen to

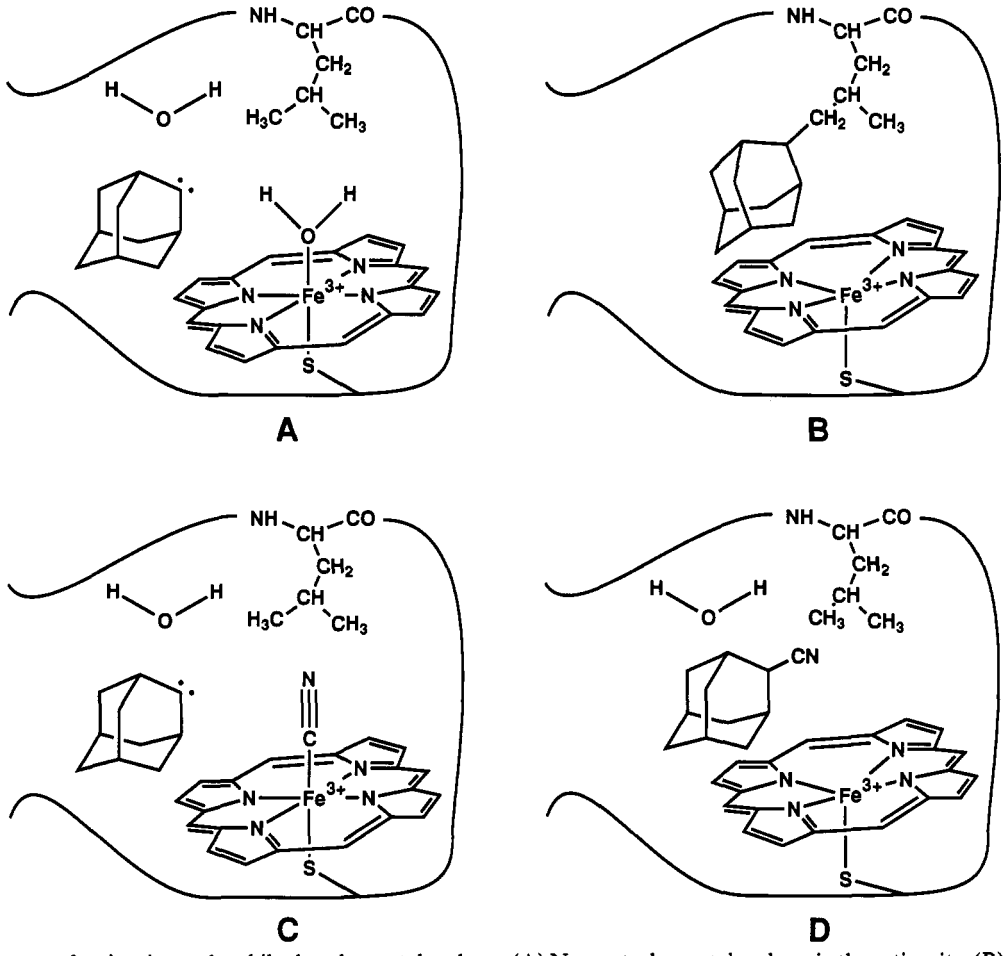

FIGURE 8: Capture of active site nucleophiles by adamantyl carbene. (A) Nascent adamantyl carbene in the active site. (B) Covalent attachment of the adamantyl group to an amino acid R-group, resulting in permanent occupation of the substrate binding site. (C) Nascent carbene in the active site of cyanide-ligated P450. (D) Capture of the heme cyanide ligand with active-site formation of 2-adamantanecarbonitrile.

favor selectivity of active site labeling *vs* nonspecific surface labeling. Ideally, one wants both the diazirine and the protein completely bound. However, at high concentrations of protein, the fraction of bound diazirine approaches 1, but only a small fraction of the protein is bound with diazirine. On the other hand, at high concentrations of diazirine where the protein will be fully bound, a large fraction of the diazirine will be unbound, increasing the probability of nonspecific labeling of the protein. We selected the concentration pair protein = 10 μM and diazirine = 5 μM. With those initial concentrations, the protein was about one-third bound and the diazirine was about two-thirds bound.

This high-specificity approach necessitated the use of multiple labeling cycles with substoichiometric quantities of diazirine. Although, in principle, complete protein labeling can be achieved by this procedure, a practical limit is reached because of accumulation of 2-adamantanol and methanol, both of which are inhibitory to diazirine binding. Nonetheless, the extent of photolabeling achieved in this work (as high as 76%) compares favorably with those reported by others. For instance, at low reagent-to-protein ratios similar to that used here, Frey *et al.* (1986) obtained 18% labeling, while Swanson and Dus (1979) reported 45%. Yun *et al.* (1992) observed 59% labeling, but only at a ratio of 800:1. Thus, the procedure outlined here may represent a significant advance in photolabeling methodology.

Specificity of Covalent Attachment of the Adamantyl Residue to P450 2B4. Six independent criteria established that the photolabeling of P450 2B4 was nearly exclusively confined to the active site. The calculated active site occupancy based on K_S considerations precluded appreciable amounts of diazirine from being available to react at other areas of the protein. Labeling was competitively inhibited by several known P450 2B4 substrates, and enzymatic activity was completely inhibited in the labeled protein. Substrate binding was completely abolished in the labeled protein, and the photolabeled protein exhibited a permanently induced type I binding difference spectrum, which could not be reversed by dialysis. Calculations of the stoichiometry of the spin-state conversion in the modified protein indicate that at least 95% of the adamantyl residues were associated with the active site. A single small peptide contained almost 80% of the radiolabel, demonstrating that attachment of the adamantyl group occurred in a very limited portion of the entire protein. Taken together, these observations indicate specific and irreversible labeling of the substrate binding site of P450 2B4.

Mechanism of Production of 2-Adamantanol. Because the large amount of 2-adamantanol produced exceeded the amount that could have been generated outside of the active site (based on K_S considerations), substantial amounts must have been formed within the active site. The active site water molecule captured by the carbene may have been the heme sixth ligand, or it may have merely been present in the active site (Figure 8A). Three levels of chemical evidence suggested that the aquo heme sixth ligand was captured by the carbene. First, loss of the aquo ligand in the ferrous state reduced the amount of 2-adamantanol produced. Second, replacement of the heme ligand with either cyanide or carbon monoxide

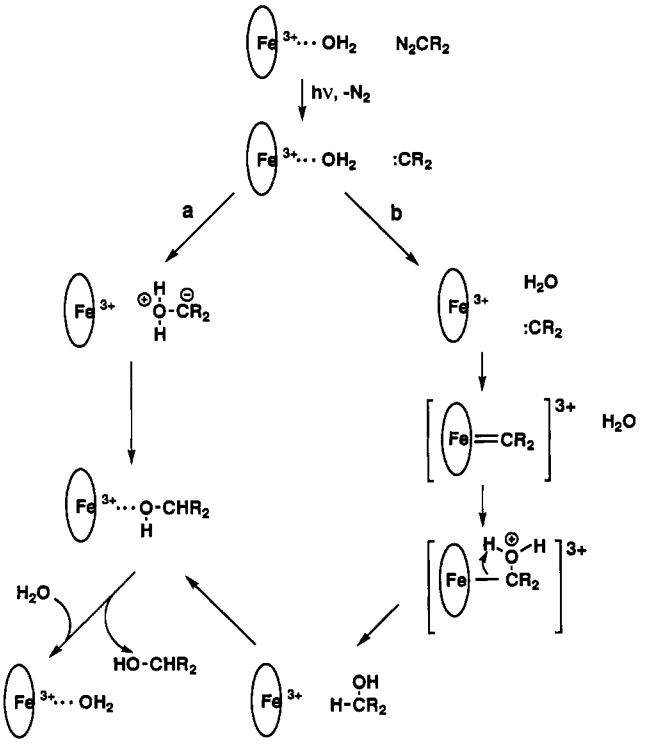

FIGURE 9: Pathways for P450 heme-assisted production of 2-adamantanol. The ellipses centered on the iron atom represent protoporphyrin IX, while N_2CR_2 and $:CR_2$ represent adamantyl diazirine and adamantyl carbene, respectively. Following photolysis of the active site diazirine, the carbene may directly attack the heme-coordinated water molecule (pathway a) or replace the water as the iron ligand (pathway b). The iron/carbene complex could react with a water molecule with net addition to yield 2-adamantanol.

reduced the amount of 2-adamantanol even further. Third, cyanide was captured to produce 2-adamantanecarbonitrile (Figure 8C,D). Cyanide capture only occurred in the presence of protein, showing that the heme–protein provides a special mechanism for delivering the cyanide to the carbene (*i.e.*, ligand capture).

A second possibility for production of 2-adamantanol in the active site is that the adamantyl carbene formed a porphyrin/iron/carbene complex (Figure 9, pathway b) similar to that obtained by the oxidation of 1,3-benzodioxazole by P450 (Mansuy *et al.*, 1979). Ortiz de Montellano and Reich (1986) have proposed that such carbene/heme complexes may react with water to yield the corresponding alcohol. Either of the two pathways, reaction of the carbene with a heme-bound nucleophile or reaction of a nucleophile with the heme-bound carbene, would serve as a P450-dependent mechanism for delivery of nucleophiles to the active site carbene. However, we favor the pathway of direct capture of heme ligands by a free carbene for the following reasons. One, an iron/carbene complex could form with either the native ferric or the ferrous enzyme, but it is unlikely that the strong ligands CN^- and CO could be displaced by the carbene. Therefore, only the ligand capture mechanism is a viable explanation for the formation of 2-adamantanecarbonitrile. Two, adamantyl carbene, because of the close contacts between its bridgehead hydrogens and the planar porphyrin ring, seems unlikely to be able to approach the iron close enough to form the expected short Fe=C bond. Three, the ferrous enzyme should have more readily formed the carbene complex than the ferric enzyme, and protein labeling should have decreased. Instead, it increased. These arguments indicate that an iron/carbene complex is not the pathway for active site production of 2-adamantanol.

Some nonligand water must have been captured in the active site as well. We can estimate the amount of active site water capture by considering the excess 2-adamantanol produced over that expected on the basis of free diazirine. For example, in the ferric case, total adamantanol production was 80%, but only 33% would have been expected due to the unbound diazirine. The excess (47%) may be attributed to water captured within the active site. When cyanide replaces water as the iron axial ligand, eliminating capture of ligand water as a means of formation of adamantanol, adamantanol production drops by only 11%. Thus, three populations of water appear to react with adamantyl carbene to produce adamantanol: ligand water, unbound active site water, and bulk solvent water. These account for approximately 11%, 36%, and 33%, respectively, of the total carbene flux. When cyanide was the iron ligand, the fraction of carbene capture of the ligand decreased to 6%, with a corresponding increase of protein capture from 6% to 10%. In other words, with one pathway of active site carbene reaction eliminated, more protein was captured. Of course, aquo ligand capture was partly replaced by cyanide ligand capture. In the ferrous carbonyl case, where the fraction of ligand capture dropped to zero, protein capture increased further to 12%.

The large fraction of carbene flux that goes to the production of 2-adamantanol demonstrates that the principal nucleophile present in the P450 2B4 active site is water, and it appears to be present in the active site in both heme-ligated and unbound states. Thus, the apparent low efficiency of photolabeling of active site residues is due to the poor ability of protein nucleophiles to compete with active site water for reaction with the photocarbene. It should be emphasized that this water is present in the active site at the same time as the bulky adamantane diazirine and, presumably, most substrates as well. This result demonstrates that, like the bacterial and mitochondrial forms of cytochrome P450, mammalian liver microsomal P450 has readily accessible water molecules present in the active site during substrate oxidation. These water molecules may be involved in providing protons during reduction of oxygen or in modulating the polarity of the active site microenvironment.

REFERENCES

Bayley, H. (1983) Photogenerated Reagents in Biochemistry and Molecular Biology, in *Laboratory Techniques in Biochemistry and Molecular Biology*, 2nd ed., Vol. 12, Elsevier, Inc., New York.

Bayley, H., & Knowles, J. R. (1980) *Biochemistry 19*, 3883–3892.

CaJacob, C. A., Chan, W. K., Shephard, E., & Ortiz de Montellano, P. R. (1988) *J. Biol. Chem. 263*, 18640–18649.

Chan, W. K., Sui, Z., & Ortiz de Montellano, P. R. (1993) *Chem. Res. Toxicol. 6*, 38–45.

Cochin, J., & Axelrod, J. (1959) *J. Pharmacol. Exp. Ther. 125*, 105–110.

Coon, M. J., van der Hoeven, T. A., Dahl, S. A., & Haugen, D. A. (1978) *Methods Enzymol. 52*, 109–117.

Dawson, J. H. (1988) *Science 240*, 433–439.

French, J. S., & Coon, M. J. (1979) *Arch. Biochem. Biophys. 195*, 565–577.

Frey, A. B., Kreibach, G., Wadhera, A., Clarke, L., & Waxman, D. J. (1986) *Biochemistry 25*, 4797–4803.

Gerber, N. C., & Sligar, S. G. (1992) *J. Am. Chem. Soc. 114*, 8742–8743.

Grab, L. A., Swanson, B. A., & Ortiz de Montellano, P. R. (1988) *Biochemistry 27*, 4805–4814.

Groves, J. T., & Watanabe, Y. (1988) *J. Am. Chem. Soc. 110*, 8443–8452.
Halpert, J. R., & He, Y. (1993) *J. Biol. Chem. 268*, 4453–4457.
Hopkins, N. E., Foroozesh, M. K., & Alworth, W. L. (1992) *Biochem. Pharmacol. 44*, 787–796.
Imai, Y., & Nakamura, M. (1991) *J. Biochem. (Tokyo) 110*, 884–888.
Jacobs, R. E., Singh, J., & Vickery, L. E. (1987) *Biochemistry 26*, 4541–4545.
Jefcoate, C. R. (1978) *Methods Enzymol. 52*, 258–279.
Kronbach, T., Kemper, B., & Johnson, E. F. (1991) *Biochemistry 30*, 6097–6102.
Mansuy, D., Battioni, J.-P., Chottard, J.-C., & Ullrich, V. (1979) *J. Am. Chem. Soc. 101*, 3971–3973.
Matsunaga, E., Zeugin, T., Zanger, U. M., Aoyame, T., Meyer, U. A., & Gonzalez, F.J. (1990) *J. Biol. Chem. 265*, 17197–17201.
McCarthy, M.-B., & White, R. E. (1983) *J. Biol. Chem. 258*, 9153–9158.
Nash, T. (1953) *Biochem. J. 55*, 416–421.
Nelson, D. R., Kamataki, T., Waxman, D. J., Guengerich, F. P., Estabrook, R. W., Feyereisen, R., Gonzalez, F. J., Coon, M. J., Gunsalus, I. C., Gotoh, O., Okuda, K., & Nebert, D. W. (1993) *DNA Cell. Biol. 12*, 1–51.
Nelson, D. R., & Strobel, H. W. (1989) *Biochemistry 28*, 656–660.
Obach, R. S., Spink, D. C., Chen, N., & Kaminsky, L. S. (1992) *Arch. Biochem. Biophys. 294*, 215–222.
Ohnishi, T., Miura, S., & Ichikawa, Y. (1993) *Biochim. Biophys. Acta 1161*, 257–264.
Oldenziel, O. H., van Leusen, D., & van Leusen, A. M. (1977) *J. Org. Chem. 42*, 3114–3118.
Ortiz de Montellano, P. R., Mathews, J. M., & Langry, K. C. (1984) *Tetrahedron 40*, 511–519.
Ortiz de Montellano, P. R., & Reich, N. O. (1986) Inhibition of Cytochrome P-450 Enzymes, in *Cytochrome P-450. Structure, Mechanism, and Biochemistry* (Ortiz de Montellano, Paul R., Ed.) pp 273–314, Plenum Press, New York.
Ortiz de Montellano, P. R. (1989) *Trends Pharmacol. Sci. 10*, 354–359.
Poulos, T. L., Finzel, B. C., Gunsalus, I. C., Wagner, G. C., & Kraut, J. (1985) *J. Biol. Chem. 260*, 16122–16130.
Raag, R., & Poulos, T. L. (1991) *Biochemistry 30*, 2674–2684.
Ravichandran, K. G., Boddupalli, S. S., Hasemann, C. A., Peterson, J. A., & Deisenhofer, J. (1993) *Science 261*, 731–736.
Shimizu, T., Sadeque, A. J. M., Sadeque, G. N., Hatano, M., & Fujii-Kuriyama, Y. (1991) *Biochemistry 30*, 1490–1496.
Stearns, R. A., & Ortiz de Montellano, P. R. (1985) *J. Am. Chem. Soc. 107*, 234–240.
Stetter, A. H., & Tilmanns, V. (1972) *Chem. Ber. 105*, 735–739.
Swanson, R. A., & Dus, K. M. (1979) *J. Biol. Chem. 254*, 7238–7246.
Swanson, B. A., Halpert, J. R., Bornheim, L. M., & Ortiz de Montellano, P. R. (1992) *Arch. Biochem. Biophys. 292*, 42–46.
Tarr, G. E., Black, S. D., Fujita, V. S., & Coon, M. J. (1983) *Proc. Natl. Acad. Sci. U.S.A. 80*, 6552–6556.
Tuck, S. F., & Ortiz de Montellano, P. R. (1992) *Biochemistry 31*, 6911–6916.
Wagner, G. C., Perez, M., Toscano, W. A., Jr., & Gunsalus, I. C. (1981) *J. Biol. Chem. 256*, 6262–6265.
White, R. E., & Coon, M. J. (1982) *J. Biol. Chem. 257*, 3073–3083.
White, R. E., & McCarthy, M.-B. (1986) *Arch. Biochem. Biophys. 246*, 19–32.
White, R. E., McCarthy, M.-B., Egeberg, K. D., & Sligar, S. G. (1984) *Arch. Biochem. Biophys. 228*, 493–502.
White, R. E., Miller, J. P., Favreau, L. V., & Bhattacharyya, A. (1986) *J. Am. Chem. Soc. 108*, 6024–6031.
Wright, G. D., & Honek, J. F. (1992) *Bioorg. Med. Chem. Lett. 2*, 383–386.
Yao, K. Q., Falick, A. M., Patel, N., & Correia, M. A. (1993) *J. Biol. Chem. 268*, 59–65.
Yun, C. H., Hammons, G. J., Jones, G., Martin, M. V., Hopkins, N. E., Alworth, W. L., & Guengerich, F. P. (1992) *Biochemistry 31*, 10556–10563.